Science World Journal Vol. 20(No 1) 2025 https://dx.doi.org/10.4314/swj.v20i1.60
www.scienceworldjournal.org
ISSN: 1597-6343 (Online), ISSN: 2756-391X (Print)
Published by Faculty of Science, Kaduna State University

Full Length Research Article

A PRELIMINARY ASSESSMENT OF NORTH-EASTERN NIGERIA'S GEOTHERMAL POTENTIAL ZONES USING LAND SURFACE TEMPERATURE

*[1,2]Usman Ahmed Kehinde; [1]Osumeje Joseph; [1]Lawal Kolawole; [1]HassanYusuf Adigun; [1]Umar Mahmood

[1]Department of Physics, Faculty of Physical Sciences, Ahmadu Bello University, Zaria, Nigeria
[2]Department of Applied and Environmental Geophysics, Faculty of Natural Sciences, Comenius University, Bratislava, Slovakia

*Corresponding Author Email Address: ahmedkehindeusman@gmail.com, akusman@abu.edu.ng Phone: +234 8164594389

ABSTRACT
The exploration of renewable energy resources is crucial for meeting the increasing energy demands of developing regions, particularly in North-Eastern Nigeria, where energy shortages persist. This study provides a preliminary assessment of geothermal potential zones in the region by analyzing land surface temperature (LST) patterns derived from satellite-based remote sensing data. Utilizing Landsat datasets, the spatial and temporal distribution of LST was examined to identify geothermal anomalies indicative of subsurface heat sources. Key geospatial techniques, including thermal anomaly mapping and integration with geological and tectonic data, were employed to delineate areas of potential geothermal interest. Images encompassing the study area were obtained and processed using ArcGIS's raster calculator basic tool to estimate the Normalised Difference Vegetation Index (NDVI) and Land Surface Temperature (LST) of the study region. The findings revealed vegetation covers that can be used as an indicator of geothermal surface manifestation by assessing the leaf condition associated with the geothermal system below the surface. Geothermal anomalies were suggested by the data, which showed little vegetation and a high temperature of roughly 24 °C throughout the study area. Results highlight several hotspots, particularly along fault zones and regions with volcanic features, which align with areas of known tectonic activity. These findings suggest a promising potential for geothermal energy exploration in North-Eastern Nigeria, offering a sustainable alternative to fossil fuels. Further geophysical investigations and field studies are recommended to validate these preliminary findings and assess the feasibility of harnessing geothermal energy in the identified zones. This research provides a foundation for renewable energy exploration in North-Eastern Nigeria, offering valuable insights for sustainable energy development in the region, and contributes also to the growing body of research on renewable energy resources in Sub-Saharan Africa and underscores the importance of geothermal energy as a viable solution for sustainable development in the region.

Keywords: *Landsat 9, Geothermal, Geospatial, NDVI, LST*

INTRODUCTION

The need for development can be achieved through the availability of sufficient energy or energy source (Cole, 2014). Energy can also be generated from earth's subsurface in form of geothermal (Lawal *et al.*, 2018). Geothermal energy is a clean energy source (Sunday, 2015) and has been exploited by several developed countries like United States of America, Indonesia, Philippines, Turkey, New Zealand etc. (Usman et al., 2025).

Nigeria does not generate enough energy for the country's overall consumption despite the country's continued population growth and the need for more power for both residential and industrial use. Although geothermal energy has been gradually incorporated into some African and global countries, Nigeria cannot be completely excluded from the possibility of investigating geothermal energy (Ewa and Kryrowska, 2010). There has ever been a more pressing need to investigate the generation of electric power from other sources to complement the ones being used. According to Lawal et al. (2018), geothermal energy is the utilization of heat energy within the earth, whereby the earth's heat engine is powered by the cooling of the crust and the heating of the lower crust and mantle by thermal decay of radioactive isotopes. As a result, the temperature rises with depth below the surface. Because energy is essential for socioeconomic development and the eradication of poverty, access to clean energy services is a significant challenge facing the African continent (Oyedepo, 2012). It has been reported by many researchers that geothermal energy is a clean and sustainable energy source, contained in intense heat, that continually flows outward from deep within the earth's core (Hulen and Wright, 2001; Nemzer et al., 2004; Nemzer et al., 2009; Obande et al., 2014; Sunday, 2015). It utilizes the earth's natural heat by sourcing superheated water found in joints and fractures in the earth's crust (Abraham, 2011; Lawal *et al.*, 2018). According to Nemzer et al. (2009), GEA (2012), and GRC (2017), the geothermal energy resource is greater than the combined resources for coal, petroleum, natural gas and Uranium. Geothermal energy is useful in heat pumps, geothermal direct heating, and power generation (Bowyer et al., 2011; Renewable Energy World, 2019).

Because the predicted heat extraction from geothermal power is negligible in comparison to the heat content of the Earth, it is seen as renewable and sustainable (Fridleifsson et al., 2008). Furthermore, geothermal energy is seen to offer significant potential for mitigating global warming due to its minimal emissions (Turcotte and Schubert, 2002). According to the World Energy Council website, Nigeria produces 4.39 megatons of gas and 120 million tons of oil annually (World Energy Council, 2014). It is therefore necessary to counter the effects of greenhouse gases produced in the country, which are dangerously high due to the high production of million/mega tons of oil and gas and the high consumption of these because of insufficient electricity supply (Usman et al., 2025). Since the technology and equipment used in the production of geothermal energy are quite like those used in the oil and gas industries, the idea of using renewable energy should be strongly supported throughout the nation. Therefore, developing its geothermal resources will be extremely

Science World Journal Vol. 20(No 1) 2025 https://dx.doi.org/10.4314/swj.v20i1.60
www.scienceworldjournal.org
ISSN: 1597-6343 (Online), ISSN: 2756-391X (Print)
Published by Faculty of Science, Kaduna State University

advantageous for Nigeria, an oil-rich region (Cole, 2014; Usman et al., 2025). It is necessary to first identify appropriate locations for the exploitation of geothermal (GT) resources. Remote sensing has proven to be an invaluable step in the pre-feasibility stages of the process because it can narrow targets before conducting a substantial survey, which allows for cost-effective coverage of large areas (Usman et al., 2023). The objective of this study is to estimate the Normalized Difference Vegetation Index (NDVI) and Land Surface Temperature (LST) to enhance and identify geothermal potential zones using Landsat 9. Thermal infrared (TIR) remote sensing data (Landsat 8 satellite data) is used to map and quantify temperature anomalies associated with surface geothermal features such as fumaroles, and steaming ground, which comes from the subsurface of the area reach the ground by conduction and convection (Claudia and Stefan, 2013). The Thermal Infrared Sensor (TIRS) and the Operational Land Imager (OLI) are its two distinguishing sensors, according to Storey et al. (2014).

MATERIALS AND METHODS

Description of Study Area and Geothermal Implications

The study area (Figures 1a&b) is bounded by latitudes 9˚30′00′′ N – 14˚0′00′′ N and longitudes 9˚0′00′′ E – 14˚30′00′′ E and comprises Adamawa, Bauchi, Borno, Gombe, Taraba, and Yobe states and part of north central states like Plateau state in the northern part of Nigeria. The area comprises three major groups of rocks, namely the Precambrian Basement Complex, Cretaceous Sediments, and Tertiary/Quaternary volcanic rocks of the Biu Plateau (Jalo, 2015). In the late 1980s through 1990s, the Basement Complex of northeastern Nigeria and, to some extent, the Cretaceous sediment in the region were studied concerning the favorability, structural settings, and geochemistry of uranium (U) mineralization (Funtua et al., 1999; Jalo, 2015). Numerous low-grade uranium mineralizations occur within the Gubrunde horst (basement complex) and in the sedimentary rocks adjacent to the Peta syncline. Other U mineralization include those of Ghumchi and Mika (Dada and Suh, 2006). The mineralization commonly occurs in fractured, sheared or brecciated zones of granites which are sometime in association with later rhyolites. (Islam and Baba, 1990). The presence of hot springs and basins, the Tertiary and Quaternary volcanic rocks, and U mineralization in north-eastern Nigeria are all good geological evidence of potential geothermal energy.

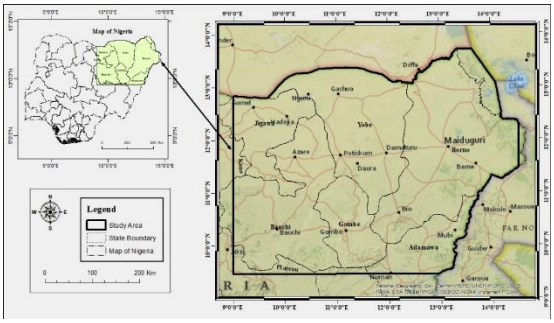

Figure 1(a): Geological map of Nigeria showing the proposed study area (Usman et al., 2025 as digitized)

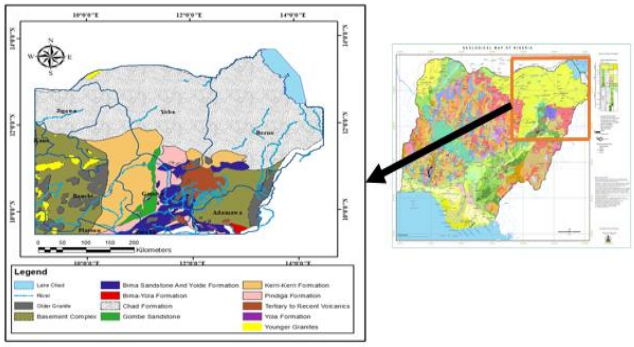

Figure 1(b): Geological map of the study area (Adapted From NGSA, 2009)

Remote Sensing Data

Detection and discrimination of objects or surface features mean detecting and recording radiant energy reflected or emitted by objects or surface material (Figure 2). Remote sensing has to do with the emission of electromagnetic radiation (EMR), whereby energy is transmitted from the source to the surface of the earth, as well as absorption and scattering. EMR interacts with the earth's surface (reflection and emission), and then energy is transmitted from the surface to the remote sensor. Finally, sensor data output, transmission, processing, and analysis.

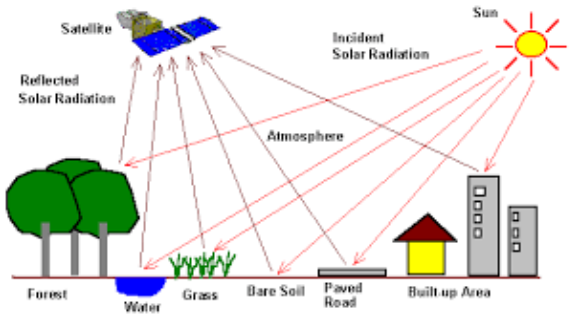

Figure 2: Remote Sensing Process (Usman et al., 2023)

A Landsat 8 level 2 image for the study area is identified as paths 184-188 and rows 050-054. The data were obtained between April 1 – May 1, 2023. The data and a metadata file contain information useful for computing Top of Atmosphere, Brightness Temperature etc. were downloaded from USGS website. The study area (according to meteorological data) has low environmental temperature (average) in April, the period the data was acquired. The choice of date of data selection considered days of less heating influence from solar radiation on land surface. The Shuttle Radar Topographic Mission (SRTM) data of NASA was also primary data used for comparing regions of high LST with the topography.

Data Processing

The data considered from remotely sensed data is Landsat 8's red, near infrared and thermal infrared. Satellite TIRS sensors measure TOA radiances, which was then converted to TOA brightness temperatures using Planck's equation. The knowledge of surface emissivity is important in reducing the error in estimation of LST

Science World Journal Vol. 20(No 1) 2025 https://dx.doi.org/10.4314/swj.v20i1.60
www.scienceworldjournal.org
ISSN: 1597-6343 (Online), ISSN: 2756-391X (Print)
Published by Faculty of Science, Kaduna State University

from satellite data. Emissivity measurement is obtained from NDVI Threshold based method. Normalized Deferential Vegetative Indexes (NDVI) were derived from atmospherically corrected bands 4 and 5 data. This result was used as an input to calculate fractional vegetation cover. It is the most important parameter to measure surface emissivity from remotely sensed data.

Imageries of the same band were combined (mosaic) to get a single mosaic raster for the band, and this was achieved for bands 4, 5, 10, and 11. The service provider, USGS, had already performed geometric and reflectance corrections for the L2 data type, which is orthorectified (terrain corrected). The raster calculator basic tool option in ArcGIS was used to make the calculations. The NDVI and land surface temperature of the study area were estimated using spatial analysis algorithm as explained below.

Top of Atmosphere (TOA), L: TOA (L) reflectance is the reflectance measured by a space-based sensor flying higher than the earth's atmosphere. It is calculated as:

$$L = (M_L \times Q) + A_L \quad (1)$$

$$M_L = Radiance\ MULT\ Band\ 10\ value$$
$$A_L = Radiance\ ADD\ Band\ 10\ value$$
$$Q = Mosaic\ raster\ of\ Band\ 10$$

The following table (table 1) lists two sets of M_L and A_L for band 4, 5, 10 and 11 from metadata file of an image.

Table 1: LANDSAT 8 Radiance Scale Factors

BAND NUMBER	M_L	A_L
BAND 4	9.7443E-03	-48.72136
BAND 5	5.9630E-03	-29.81504
BAND 10	3.3420E-04	0.10000
BAND 11	3.3420E-04	0.10000

Brightness Temperature (BT): This is a measurement of the radiance of the microwave radiation traveling upward from the top of the atmosphere to the satellite.

$$BT = K_2/(\ln(\frac{K_1}{L} + 1) - 273.5 \quad (2)$$

$K_2 = Constant\ 2\ Band\ 10\ value$, $K_1 = Constant\ 1\ Band\ 10\ value$ (table 2)

Table 2: Thermal constant value of K_1 and K_2

Thermal Constant	Band 10	Band 11
K_1	774.8853	1321.0789
K_2	480.8883	1201.1442

Normalized Difference Vegetation Index (NDVI): This is derived from the visible near-infrared bands. NDVI is an indicator that describes the greenness – the relative density and health of vegetation. Areas of bare rock, sand, or snow typically have very low NDVI values (0.1 or less), with NDVI values ranging from +1.0 to -1.0 (Sobrino and Raissouni, 2000). Low levels of vegetation, such as shrubs and grasslands, or failing crops can result in moderate NDVI values (around 0.2 to 0.5). High NDVI values (between 0.6 and 0.9) are indicative of thick vegetation, like that found in tropical and temperate woods, or peak development stages of crops. The NDVI was computed using the float option with mosaic bands 4 and 5 as follows:

$$NDVI = \frac{Band\ 5 - Band4}{Band\ 5 + Band\ 4} \quad (3)$$

Proportion of Vegetation (P_V): Maximum and minimum estimated values of NDVI were used to calculate P_V as:

$$P_V = square(\frac{NDVI - NDVI_{min}}{NDVI_{max} - NDVI_{min}}) \quad (4)$$

Emissivity (ϵ): Emissivity is the measure of an object's ability to emit infrared energy and emitted energy indicates the temperature of the object.

$$\epsilon = 0.004 \times P_V + 0.986 \quad (5)$$

Land Surface Temperature (LST): LST is simply a measurement of how hot the land is. It is estimated as follows:

$$LST = (\frac{BT}{1 + \left(W \times \frac{BT}{P}\right) \times \ln(\epsilon)})$$

$$LST = (\frac{BT}{1 + \left(0.00115 \times \frac{BT}{1.4395}\right) \times \ln(\epsilon)}) \quad (6)$$

$$w = wavelenght\ of\ emitted\ radiance = 11.5\mu m$$
$$P = \frac{hc}{s} = 1.4395 \times 10^{-2}\ mK$$
$$h = Planck's\ constant\ (6.626 \times 10^{-34}\ Js)$$
$$c = Velcoity\ of\ light\ (2.998 \times 10^{8}\ m/s$$
$$s = Boltzmann\ constant\ (1.38 \times 10^{-23}\ J/K)$$

FINDINGS AND DISCUSSION

The results of the mosaic bands 4, 5, 10 and 11 are summarized in Table 3 below, and their respective maps are as shown in Figures 3 (a-d).

Science World Journal Vol. 20(No 1) 2025 https://dx.doi.org/10.4314/swj.v20i1.60
www.scienceworldjournal.org
ISSN: 1597-6343 (Online), ISSN: 2756-391X (Print)
Published by Faculty of Science, Kaduna State University

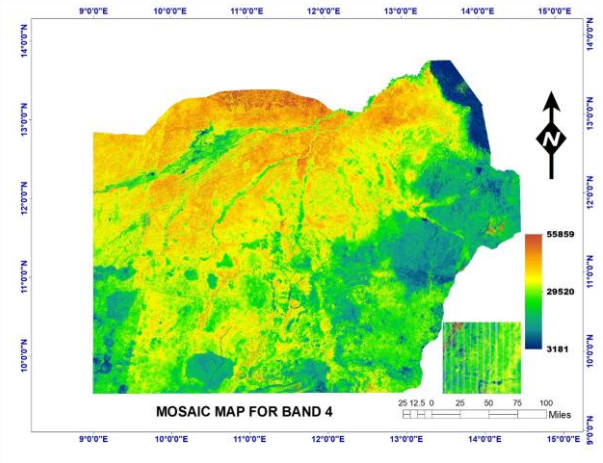

Figure 3a: Mosaic Map for Band 4

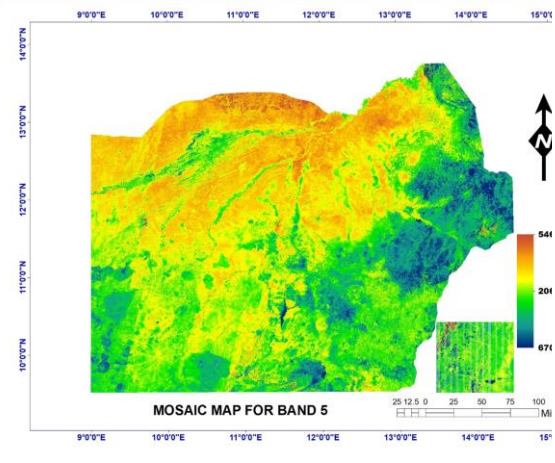

Figure 3b: Mosaic Map for Band 5

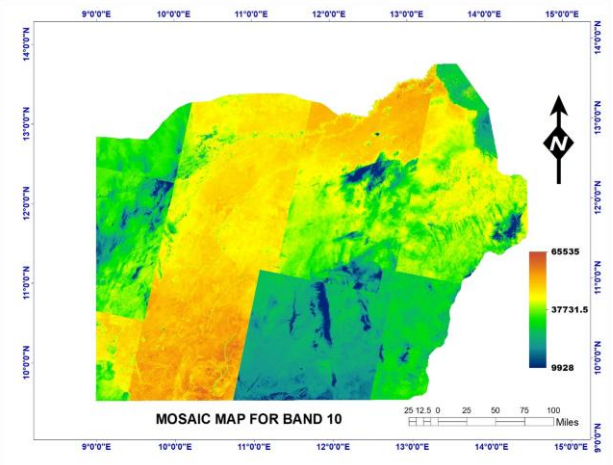

Figure 3c: Mosaic Map for Band 10

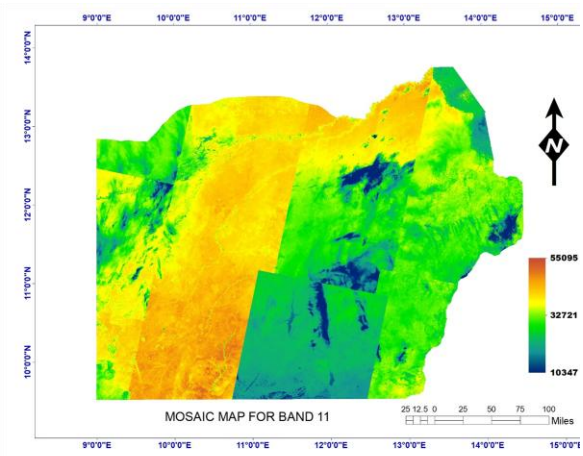

Figure 3d: Mosaic Map for Band 11

Table 3: Statistics of mosaic images for bands 4, 5, 10 and 11

Band/Parameter	Minimum	Maximum	Mean	SD
Band4	3181	55859	15266.3	2250.22
Band 5	6706	54617	19741.7	2654.46
Band 10	9928	65545	32315.5	3553.31
Band 11	10347	55095	29215.0	2793.12

The computed TOA for band 10 ranges from 3.417938 to 22.001799 while the TOA for band 11 ranges from 3.557967 to 18.512751 and their respective maps are displayed in Figures 4 (a & b). The mean of TOA computed using cell statistics algorithm ranges from 3.515858 to 20.257275 with a mean of 10.381756 and its map displayed in Figure 5.

Science World Journal Vol. 20(No 1) 2025 https://dx.doi.org/10.4314/swj.v20i1.60
www.scienceworldjournal.org
ISSN: 1597-6343 (Online), ISSN: 2756-391X (Print)
Published by Faculty of Science, Kaduna State University

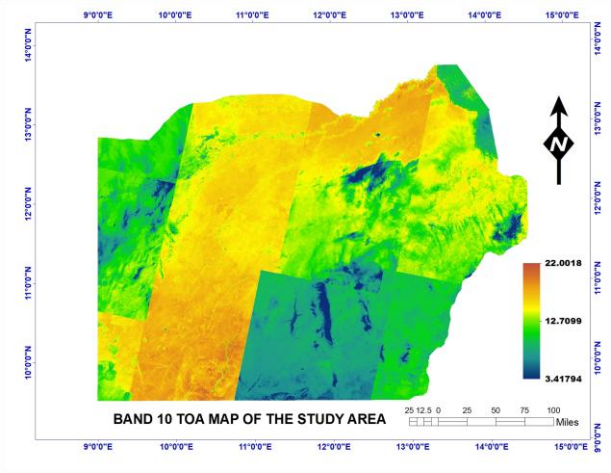

Figure 4a: TOA Map for Band 10

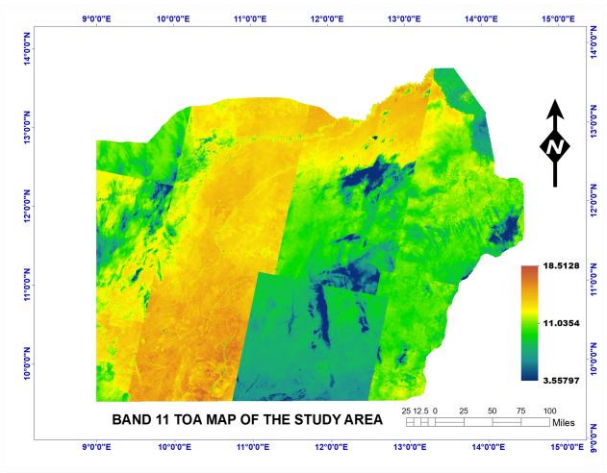

Figure 4b: TOA Map for Band 11

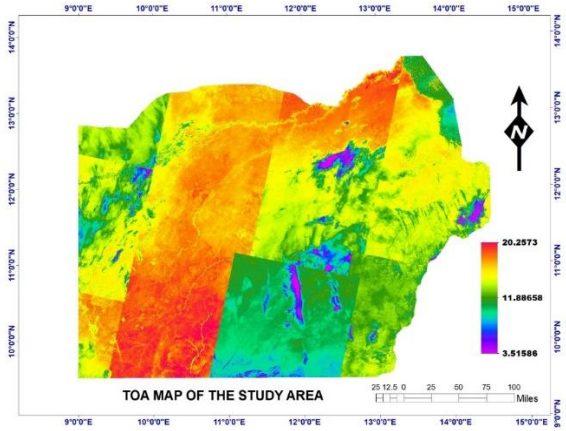

Figure 5: The Mean of Top of Atmosphere Map of the Study Area

The estimated values of BT for band 10 ranges from -30.121292 ℃ to 94.530701 ℃ while the BT for band 11 ranges from -29.057816 ℃ to 91.040955 ℃ and their respective maps are displayed in figures 6 (a & b). The mean of BT estimated using cell statistics algorithm ranges from -29.210159 ℃ to 92.785828 ℃ with a mean of 34.402740 ℃ and its map displayed in figure 7.

Science World Journal Vol. 20(No 1) 2025 https://dx.doi.org/10.4314/swj.v20i1.60
www.scienceworldjournal.org
ISSN: 1597-6343 (Online), ISSN: 2756-391X (Print)
Published by Faculty of Science, Kaduna State University

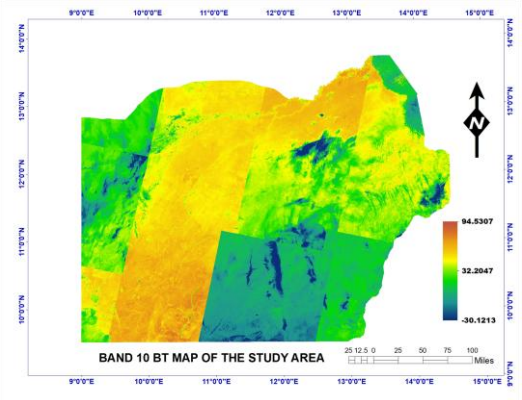

Figure 6a: BT Map for Band 10

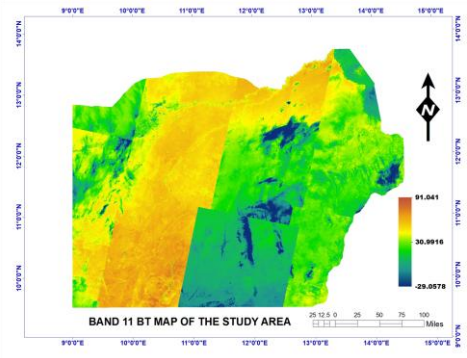

Figure 6b: BT Map for Band 11

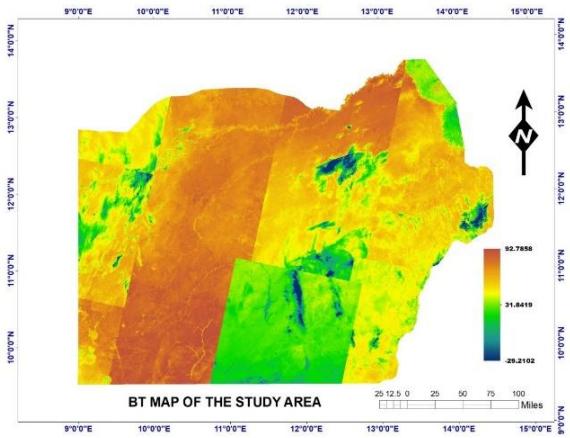

Figure 7: The Mean of Brightness Temperature Map of the Study Area

The result of the NDVI computed is shown in Figure 8. The estimated values range between -0.19 and 0.50 with a mean of 0.13 and standard deviation of 0.03. The NDVIs (lowest NDVI pixels with the lowest frequency) is -0.191956 while NDVIv (highest NDVI pixels with the highest frequency) is 0.500799. These values were used as input to derive P_V.

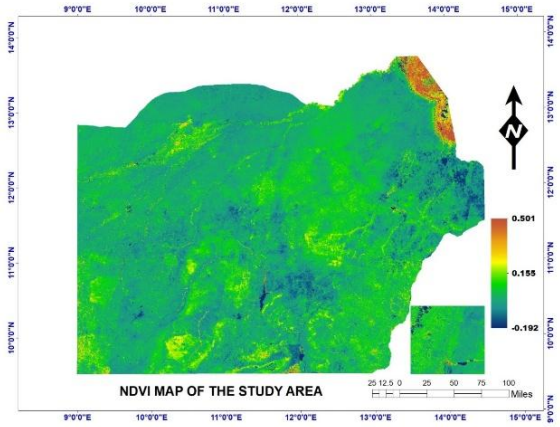

Figure 8: NDVI Map of the Study Area

The proportion of vegetation (P_V) of the study area was computed and the map is shown in Figure 9. This represents the area in terms of percentage in the vertical projection of vegetation per unit area. The P_V result values range from 0 to 1 with a mean of 0.2 and standard deviation of 0.04. Zero value means the area is covered by soil and 1 value means the area is densely covered by vegetation/forest. Values in between 0 and 1 represent the extent of vegetation occupying the ground area in the vertical projection.

Science World Journal Vol. 20(No 1) 2025 https://dx.doi.org/10.4314/swj.v20i1.60
www.scienceworldjournal.org
ISSN: 1597-6343 (Online), ISSN: 2756-391X (Print)
Published by Faculty of Science, Kaduna State University

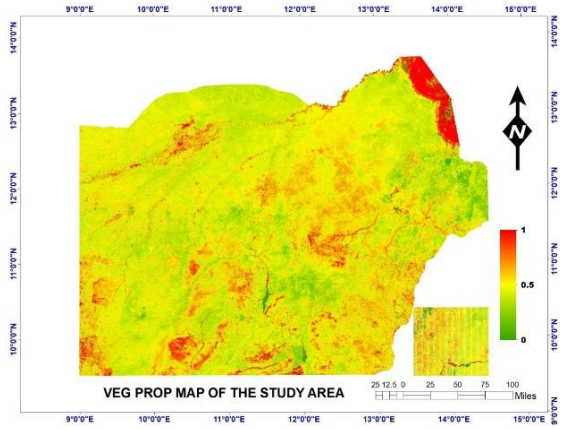

Figure 9: The Proportion of Vegetation Map of the Study Area

Land surface emissivity (LSE, ϵ) was computed using Equation 5. The computed values range from 0.986000 to 0.990000 with a mean of 0.986889. The LSE map is shown in Figure 10

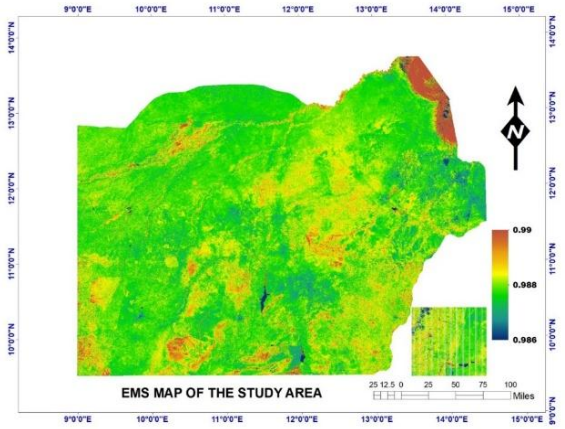

Figure 10: The Land Surface Emissivity Map of the Study Area

The LST of the study area was derived from LSE and BT. The computed values of LST for band 10 ranges from --29.841314 ℃ to 89.099686 ℃ and the values for band 11 ranges from -28.775944 ℃ to 86.473999 ℃, and their respective maps are displayed in Figures 11 (a & b). The mean of LST estimated using cell statistics algorithm ranges from -28.930748 ℃ to 87.682060 ℃ with a mean of 33.405356 ℃. The mean LST map showing the temperature distribution of the study area is as shown in Figure 12.

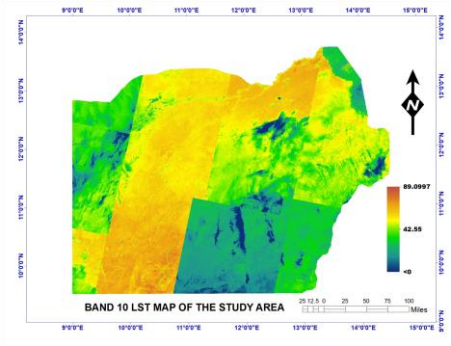

Figure 11a: LST Map for Band 10

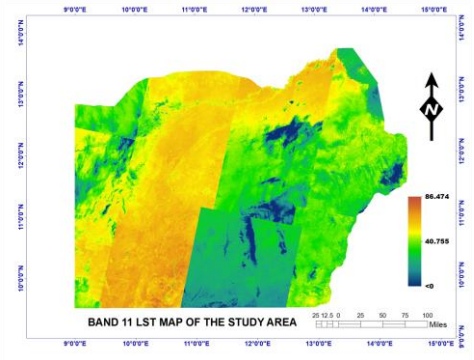

Figure 11b: LST Map for Band 11

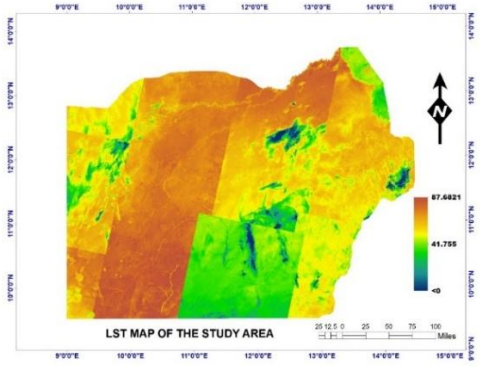

Figure 12: The Land Surface Temperature map of the study area

DISCUSSION

This study utilized Landsat imagery to analyze the thermal characteristics of the study area using Bands 4, 5, 10, and 11. The mosaic maps reveal significant variations in reflectance values, indicating heterogeneous surface conditions. Mean reflectance values for Bands 4 and 5 highlight the diversity in land cover, while the thermal bands exhibit high radiometric values, suggesting substantial spatial variability. The Top of Atmosphere (TOA) maps further establish a baseline for radiance across the area. Additionally, the derived Brightness Temperature (BT) maps display a wide range of temperatures, which, when combined with the Land Surface Temperature (LST) maps, reveal distinct thermal zones across the region.

The NDVI map, with values ranging from –0.19 to 0.50 and a mean of 0.13, indicates low to moderate vegetation cover. This is corroborated by the vegetation proportion (Py) map, where an average value of 0.2 suggests that only a small fraction of the area is densely vegetated, while much of the landscape is dominated by soil or sparse vegetation. These patterns suggest that environmental factors, such as high temperatures, may inhibit dense vegetation growth. The computed Land Surface Emissivity (LSE) values, ranging from 0.986 to 0.990, align with expected values for natural surfaces, further validating the robustness of the thermal analysis.

The LST map highlights a distinct temperature gradient across the study area, with cooler regions (green/blue zones) exhibiting temperatures around 41.76°C and hotter regions (orange/red zones) reaching up to 87.68°C. This significant variation is likely influenced by differences in land cover, vegetation density, and possibly underlying geological features. Notably, areas with sparse vegetation or exposed soil tend to exhibit higher temperatures, while cooler regions are often associated with water bodies or denser vegetation. Additionally, localized thermal anomalies identified in the LST map may indicate potential geothermal activity or other subsurface heat sources

Conclusion and Recommendations

The integration of spectral, thermal, and vegetation indices reveals significant heterogeneity in both land cover and temperature distribution across the study area. The low to moderate vegetation cover influences surface thermal properties, contributing to localized thermal anomalies. The presence of distinct thermal zones, as indicated by the broad range of LST values, suggests that certain regions may be affected by geothermal activity or anthropogenic influences. These findings highlight potential geothermal energy prospects, as persistently high surface temperatures may indicate subsurface geothermal anomalies that warrant further exploration. Overall, this study provides a comprehensive assessment of surface conditions, identifying key areas for further investigation.

For future research, field validation and ground truthing are recommended, particularly in regions exhibiting pronounced thermal anomalies, to verify the remotely sensed data. Incorporating multi-temporal datasets would help capture seasonal variations and long-term trends in vegetation cover and thermal behavior. Additionally, employing advanced spectral indices, such as the Enhanced Vegetation Index (EVI), could offer deeper insights into the relationship between land cover and thermal dynamics. Targeted investigations in regions with extreme LST values are advised to determine whether the anomalies result from natural geothermal processes or human-induced changes.

Acknowledgment

The authors appreciate the support from the grants TETF/DR&D/UNI/ZARIA/IBR/2024/BATCH 8/06.

REFERENCES

Abraham, M.E. (2011). *Interpretation of Aeromagnetic Data for Geothermal Energy of Ikogosi warm Spring Area of Ekiti State, Southwestern Nigeria.* M.Sc. Thesis Dept. of Physics ABU Zaria. Unpublish M.Sc thesis.

Bowyer, D., Bratkovich, D.S, Frank, M. and Fernholz, K. (2011). Geothermal 101: *The Basics and Applications of Geothermal Energy*. Adam Zoet. 2011 Dovetail partners, Inc.

Cole, C.A. (2014). "Review of geothermal heating and cooling of buildings" 2nd climatic change technology conference.

Dada, S.S. and Suh, C.E. (2006). Finding economic uranium deposits and the Nigerian energy mix: Implications for national development. In: Abaa SI, Baba S (eds.), *Proc. first Petr. Tech. Dev. Fund (PTDF) workshop, University of Maiduguri*, pp. 34 – 48.

Ewa, K. and Kryrowska, S. (2010). Geothermal exploration in Nigeria. *Proceedings World Geothermal Congress. Zaria, Nigeria*, (3); 1 – 59.

Fridleifsson, I.B., Bertani, R., Huenges, E., Lund, J.W., Ragnarsson, A. and Rybach, L. (2008). The possible role and contribution of geothermal energy to the mitigation of climate change. *Luebeck, Germany, pp. 59–80.*

Funtua, I.I., Okujeni, C.D. and Elegba, S.B. (1999). Preliminary note on the geology and genetic model of uranium mineralization in Northeastern Nigeria. *J. Min. Geol.* 35(2):125 – 136.

GEA, (2012). Geothermal basic Questions and Answers. http://geotehrmal.org/what.html.pp8.

GRC (2017). Advancing Geothermal Development through Education Outreach and Dissemination of Research. http://geothermal.org/whathtml.

Hulen, J.B. and Wright, P.M. (2001). Geothermal Energy: Sustainable Energy for the Benefit of Humanity and the Environment. *Energy & Geoscience Institute, University of Utah.*

Islam, M.R. and Baba, S. (1990). The mineral potential of the northern part of Mandara hills, Nigeria. *Berg-und huttenmannische monatshefe (BHM)* 135(4):95 –98.

Jalo, M.E. (2015). Geology and petrography of the rocks around Gulani Area, Northeastern Nigeria. *Journal of Geology and Mining Research*,7(5), pp. 41-57.

Lawal, T. O., Nwankwo, L.I., IWA, A.A., Sunday, J.A. and Orosun, M.M. (2018). Geothermal Energy Potential of the Chad Basin, North-Eastern *Nigeria. J. Appl. Sci. Environ. Manage.* Vol. 22 (11) 1817–1824

Nemzer, M.L., Carter, A.K. and Nemzer, K.P. (2004). Geothermal energy facts: Geothermal Education Office, online at: http://geothermal.marin.org/pwrheat.html

Nemzer, M.L., Carter, A.K. and Nemzer, K.P. (2009). Geothermal Energy. Microsoft Encarta 2009 (DVD). Redmond, W.A.: Microsoft Corporation, 2008.

NGSA (2009). Nigerian Geological Survey Agency's Lineament and Geological Map of Nigeria, Scale 1:100 000.

Obande, G.E., Lawal, K.M. and Ahmed, L.A. (2014). Spectral

Analysis of Aeromagnetic Data for Geothermal Investigation of Wikki Warm Spring, North-East Nigeria. *Geothermics*, 50, 85-90.

Oyedepo, S.O. (2012). Energy and sustainable development in Nigeria: The way forward. Energy, Sustainability, and Society. 2:15.

Renewable Energy World (2019). Geothermal Energy. https://www.renewableenergyworld.com /geotehrmalenergy/tech/geoelectricity.html Copyright 1999-2019 RenewableEnergy World.com - All rights reserved.

Sobrino, J.A. and Raissouni, N. (2000). Toward remote sensing methods for land cover dynamic monitoring: Application to Morocco. *International Journal of Remote Sensing*, 21(2), 353-366. https://doi.org/10.1080/014311600210876

Storey, J., Choate, M., Lee, K. (2014). Landsat 8 Operational Land Imager on-Orbit Geometric Calibration and Performance. *Remote Sensing,* 6(11), 11127-11152.

Sunday, E.S. (2015). Renewable: Exploring Geothermal for Electrification. Daily Trust Monday, October 26. http://www.dailytrust.com.ng.

Turcotte, D. L. and Schubert, G. (2002). Geodynamics (2 ed.), Cambridge, England, UK: Cambridge University Press, pp. 136–137, ISBN 978-0-521-66624-4.

Usman A. K., Lawal K.M. and Osumeje J. (2023). A Preliminary Evaluation of Geothermal Potential Zones in North-Eastern Nigeria. *Proceedings of the 1st International Health Services Congress*. Pg. 83-89. https://tr.iksadkongre.com/library.

Usman A. K., Osumeje J., Bello Y.A.., Hassan Y.A. and Onuh E. (2025). Evaluation of Geothermal Energy Resource Potential in Northeastern Nigeria Using Spectral Analysis of Aeromagnetic Data. *Science World Journal*. Vol. 20(No 1) 2025. ISSN: 1597-6343 (Online).

World Energy Council (2014). http://www.worldenergy.org/data/trilemma index/country/Nigeria/2014/.